

Melting of the alkaline-earth metals to 80 GPa

Daniel Errandonea,^{1,*} Reinhard Boehler,¹ and Marvin Ross^{1,2}

¹Max Planck Institut für Chemie, Postfach 3060, D-55020 Mainz, Germany

²Lawrence Livermore National Laboratory, University of California, Livermore, California 94551

(Received 1 June 2001; revised manuscript received 14 September 2001; published 5 December 2001)

The melting curves of Mg, Ca, Sr, and Ba were measured in a laser-heated diamond-anvil-cell to 80 GPa. Systematic changes in the melting slopes were found to be associated with the phase transitions observed at room temperature and with the increasing *d*-electron character of these metals. Mg, Ca, and Sr show a flattening of the melting curve ($dT/dP \sim 0$) when they melt from the bcc structure, most likely due to the small volume change between bcc and melt structures. Sr exhibits a melting minimum at 40 GPa and 2000 K which is coincident with the presence of complex structures observed at room temperature. Above 20 (40) GPa, Ba (Sr) shows a continuous rise in the melting temperature apparently related to the completion of the $sp \rightarrow d$ electron transfer.

DOI: 10.1103/PhysRevB.65.012108

PACS number(s): 62.50.+p, 64.70.Dv, 71.20.Dg

The alkaline-earth metals, Group IIa in the Periodic Table, have relatively large compressibilities and phase diagrams strongly influenced by a nearly empty *d*-band lying in close proximity to the *sp*-valence band.¹ The *d*-band occupation increases with increasing atomic number, and with increasing pressure.¹ At zero pressure each of these metals may be considered as being at different stages of the high-pressure structural sequence. Under compression the structures, except for Mg, show an unusual trend in going from highly symmetric structures to more open structures. The appearance of complex structures in Ba² and Sr³ or of a simple cubic structure in Ca^{4,5} is believed to be the result of *sp**d* hybridization. In effect, pressure converts the alkaline-earth metals from an alkali metal-like to an early transition metal-like character. At much higher pressures, beyond the termination of the $sp \rightarrow d$ electron transfer,⁵ the reappearance of a close-packed structure was observed in Ba.⁶

It is well known that complex structures found in the solid are often associated with unusual features in the melting curve. The classic examples are the alkali metals, Rb and Cs, which exhibit unusual phase transitions induced by $sp \rightarrow d$ electron transfer that are associated with temperature maxima in the melting curves.⁷ Previously, the melting curves of Mg, Ca, and Sr have been studied only below 4 GPa in a piston cylinder apparatus.^{8–10} The melting temperature of Mg has been also determined by shock compression¹¹ from 40 to 50 GPa and the phase diagram of Ba has been studied to 13 GPa and 1000 K.^{8,12}

In the present work we present new melting data for the alkaline-earth metals Mg, Ca, Sr, and Ba to pressures nearly an order of magnitude greater than achieved in earlier works. Measurements were made using a laser-heated diamond-anvil-cell to pressures near 90 GPa where melting temperatures approach 3500 K. The samples were heated with a Nd:YLF laser (Quantronix, 50 W, TEM₀₀ mode, $\lambda = 1.053 \mu\text{m}$) whose defocused beam created a hot spot on the sample of about $30 \mu\text{m}$ in diameter. The temperatures were determined by an accurate fitting of the thermal emission, measured with a CCD detector from an area of $1 \mu\text{m}$ in diameter in the center of this spot, to the Planck function in the spectral range 550–800 nm.¹³ Melting was determined

using the laser speckle method.¹⁴ A detailed description of the experimental procedure is given in our recent reports for the rare earths¹⁵ and transition metals¹⁶ and elsewhere.¹⁷ Mainly, argon was used as a pressure transmitting medium in a diamond-coated tungsten gasket. In some cases the results obtained in this way are compared with those obtained using other pressure media such as Al₂O₃, KBr, or NaCl. Small samples with a stated purity higher than 99.9% (Johnson Matthey Company) and fresh surfaces were loaded in a high purity argon (99.999%) filled glove box in order to avoid oxidation of the reactive samples. The pressure and pressure gradients were determined from unheated ruby chips on the basis of the ruby pressure scale.¹⁸ After melting the samples did not show any visible indication of either oxidation or chemical reaction with the different pressure media used in this study. Figures 1–4 show the melting curves of Mg, Ca, Sr, and Ba, respectively, together with previously published results on the phase diagrams.^{8–12} Our low pressure data agree within 100 K with measurements made using a piston-cylinder apparatus.^{9,10}

Theoretical calculations¹⁹ have shown that in the polyvalent metals, Al and Mg, the almost empty *d*-electron band plays a role in determining the stable structure at high pressure. In all of the alkaline-earth metals compression induces a downward movement of the 3*d* electron energy levels increasing the *d*-character of the valence band. As a result, Mg at room temperature (RT) transforms from the hcp structure to the bcc structure at 50 GPa, with a small volume change, $\Delta V/V \sim 1\%$.²⁰ No further transitions are seen in Mg to 70 GPa.^{5,20}

Figure 1 shows the phase diagram of Mg. At low pressures, the melting slope of Mg is 6 K/GPa, very close to that of Al.²¹ Above 40 GPa the melting curve bends toward the pressure axis, becoming nearly flat above 70 GPa. Relatively small melting slopes ($dT/dP \sim 0$) are known to be characteristic of the bcc phases of the alkali, rare earth and transition metals.^{7,15,16} The reason appears to be related to the low packing efficiency of the bcc structure.¹⁶ While close-packed structures require a coordination number of 12, bcc has a coordination of 8, closer to the more open coordination of the melt. Thus, since the packing ratio for bcc (~ 0.68) is

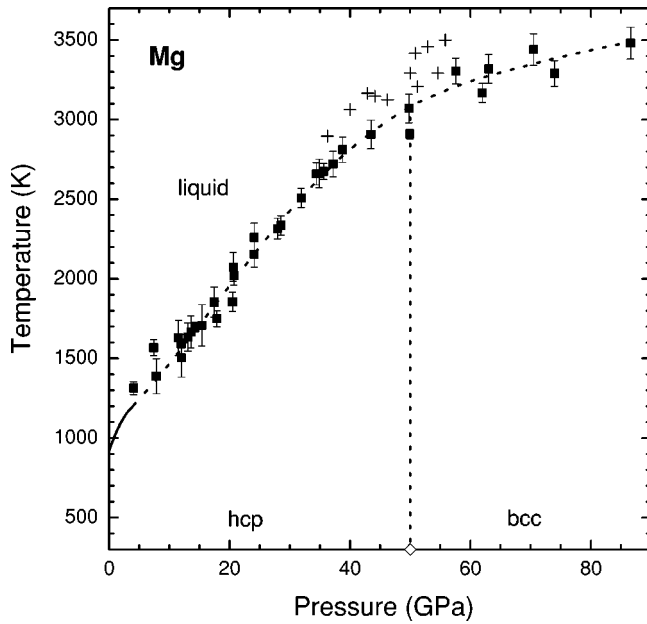


FIG. 1. Phase diagram of Mg. Solid squares correspond to the present results. The low pressure data (solid line) are taken from Ref. 9. The dotted lines are suggested phase boundaries. Crosses correspond to the shock loading data (Ref. 11). Diamonds represent the 300 K phase transitions (Ref. 20).

lower than for fcc or hcp (~ 0.74) it can be expected that the volume change (ΔV) of melting for a bcc solid to a liquid will be smaller than for a close-packed solid. Hence, it can be inferred from the Clausius–Clapeyron relation:

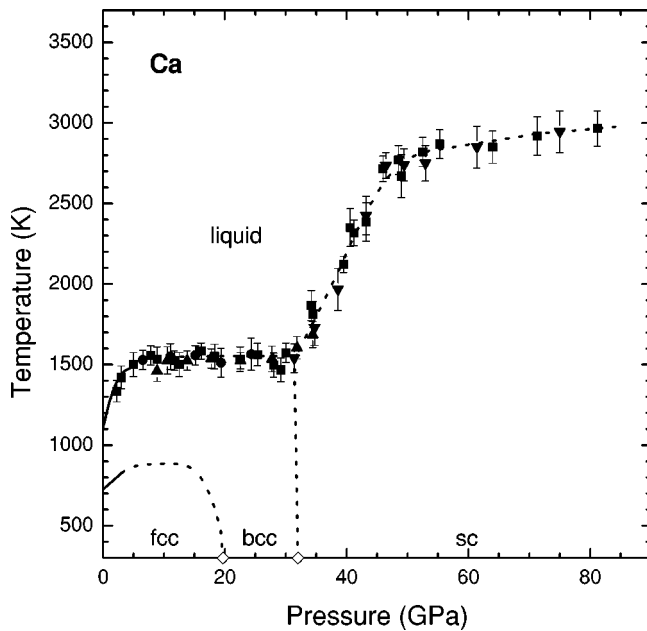


FIG. 2. Phase diagram of Ca. The present melting data were measured in different pressure media: squares (Ar), circles (KBr), down triangles (Al_2O_3), and up triangles (NaCl). Solid lines represent the piston-cylinder data (Ref. 10). The dotted lines are suggested phase boundaries. Diamonds represent the 300 K phase transitions (Ref. 4).

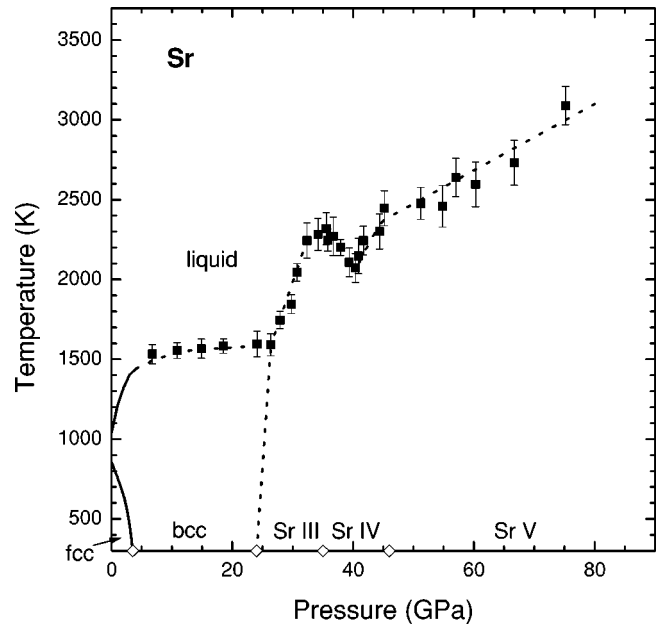


FIG. 3. Phase diagram of Sr. Solid squares represent the present melting results. Solid lines are taken from Ref. 10. The dotted lines are suggested phase boundaries. Diamonds represent the 300 K phase transitions. (Ref. 4).

$$dT/dP = \Delta V/\Delta S, \quad (1)$$

where ΔS is the entropy change, that dT/dP will be lower for bcc melting. In fact, for Ca and Sr (Figs. 2 and 3), melting from the bcc phase leads to relatively flat melting slopes ($dT/dP \sim 0$).

Since the bending of our melt line at 50 GPa is consistent with the hcp \rightarrow bcc transition pressure observed at RT by

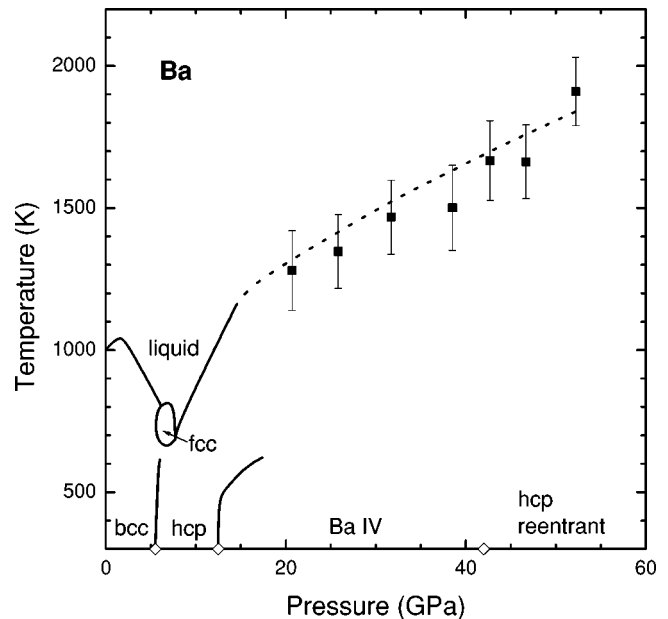


FIG. 4. Phase diagram of Ba. Solid squares represent the present melting results. The solid lines were taken from Ref. 12. Diamonds represent the 300 K phase transitions (Ref. 12).

Olijnyk and Holzapfel²⁰ we have drawn a phase line connecting our result to theirs at about 50 GPa. On the other hand, Moriarty and Althoff predicted that the hcp-bcc boundary line would be highly temperature dependent, having a negative slope and intersecting the melting curve at 1180 K and 4.3 GPa.²² In this case, a flattening of the melting curve should take place near 5 GPa which is in contradiction with the present results. This fact casts some doubts on the correctness of the theoretical predictions.²² However, the melting curve calculated in Ref. 22 is in good agreement with our measurements. The fact that the present data fail to show sharp changes in the melting slope associated with a triple point might be related with the very small volume change estimated for the hcp→bcc transition ($\Delta V/V < 0.5\%$)²³ or to the possibility of a continuous high temperature martensitic hcp→bcc transition.^{24,25} In the latter case this would imply the existence of an hcp-bcc critical point in the solid at a temperature below melting.

Shock melting temperature data for Mg¹¹ are shown by crosses in Fig. 1. These data lie systematically 200 K above of our melting curve, but follow the same trend. In Ref. 11 temperatures were estimated from the intensity of the thermal radiation measured in a narrow band in the near infrared (around 900 nm) on the assumption that the emitted radiation is that of a black body. This assumption could easily explain the differences between the shock data and the present data.

Figure 2 shows the phase diagram of Ca. At ambient conditions Ca is fcc and transforms to the bcc phase at 19.5 GPa. With increasing pressure Ca goes to a 6-fold coordinated simple cubic (sc) structure at 32 GPa accompanied by a large volume change ($\Delta V/V \sim 8\%$).⁴ This high-pressure phase is observed up to 80 GPa.⁵

At 1 bar pressure Ca melts in the bcc phase at 1100 K. The melting temperature increases gradually with increasing pressure up to 5 GPa. Above 5 GPa the melting stays flat up to about 32 GPa. This behavior is typical of bcc melting and provides additional support to the idea that the fcc→bcc transition at 19.5 GPa⁴ (where $\Delta V/V \sim 2\%$) could be connected to the low pressure and high temperature fcc→bcc transition¹⁰ (see Fig. 2), presenting a certain analogy to the low pressure part of the Sr phase diagram (see Fig. 3). This conclusion was previously inferred by observing that for both metals bcc phases have a common equation of state.⁴ Above 32 GPa a sharp increase occurs in the melting slope, which is most likely due to the large volume change associated with the transition to the simple cubic phase.⁴ We estimate the bcc-sc-liquid triple point at 32 GPa and 1550 K. The melting slope again flattens above 45 GPa and remains nearly flat up to 81 GPa, the highest pressure attained in this set of experiments. Assuming there are no additional high-temperature phases present, the melting above 32 GPa should be from the simple cubic phase. This structure (coordination number 6 and packing ratio ~ 0.52) is even more open than the bcc structure, and is consistent with the second flattening observed in the melting curve.

The Sr phase diagram is shown in Fig. 3. At RT Sr transforms from fcc to bcc at 3.5 GPa. This phase is stable to 24 GPa where there is a transition to Sr-III with a 2% volume change.⁴ With increasing pressure, at 35 GPa, a transition to

Sr-IV has been observed by high resolution x-ray studies.^{4,5,26} Finally, there is a transition to Sr-V at 46 GPa.⁴ The structure of Sr-III has been determined to be tetragonal, with the β -tin structure.²⁷ The structure of Sr-IV is complex and unknown.⁴ Sr-V (and Ba-IV) is a very unusual structure composed of a host and two or more guest components made up of incommensurate chains that lie in the channels of the host.³

The low pressure melting curve of Sr follows the same trend as in Ca, having an abrupt change of its slope at 25 GPa. Above this pressure a steep increase in the melting temperature is observed reaching a maximum at 32 GPa near the proposed onset of Sr-IV and dropping to a minimum at 40 GPa. On further compression the melting temperature increases almost linearly to 75 GPa, the highest pressure reached in our measurements. We attribute the discontinuity observed in the melting slope at 25 GPa to the intersection of the melting curve with the boundaries of the bcc and other solid phase. Since this discontinuity occurs around the same pressure as the RT bcc→Sr III transition⁴ we tentatively interpolate the RT phase boundary to the triple point (see Fig. 3) and estimate the pressure and temperature to be about 25 GPa and 1500 K. However, the shape of the melting curve suggests that there could be either a bcc-III-IV or a III-IV-V solid phase triple point between 24 and 46 GPa. The topology of the phase diagram is not clear in this region.

Since Ba is further along the $sp \rightarrow d$ transition than the lighter alkaline-earth metals it stabilizes in the bcc structure at ambient conditions and exhibits similar properties as Sr at a lower pressure. At 5.5 GPa and RT Ba transforms from bcc to a hexagonal-close-packed (hcp) structure, Ba-II.²⁸ At 12.6 GPa Ba-II transforms into the complex phase Ba-IV^{2,12} and to another hcp phase, Ba-V, at 45 GPa which is stable to at least 105 GPa.^{5,6} Ba IV is nearly identical to Sr-V.

At 1000 K Ba melts from the bcc phase. Earlier measurements have reported a negative melting slope at low pressure and the occurrence in the melting curve of a maximum at 2 GPa in the bcc phase and additional anomalies between 6 and 9 GPa.²⁹ A more recent work clarified that in this pressure region the melting curve of Ba has a minimum only near 7.7 GPa.¹² The minimum occurs just prior to the stabilization of Ba IV. The existence of the minimum¹² is believed to be due to the presence of incommensurate host-guest structure² and of a high-temperature fcc phase (Ba III). Unfortunately, our experimental method for measuring temperature using emitted radiation from very small areas is limited to temperatures above about 1100 K and for Ba melting, above 20 GPa. This prevent us from making any direct comparison with the low-pressure melting experiments and establishing a clearer connection between the RT structural sequence and the phases near melting. However, the melting temperature of Ba above 7.7 GPa increases with increasing pressure^{5,29} and an extrapolation to higher pressure is in good agreement with our data above 20 GPa.

The steep melting slope of Ba and Sr at high pressure can be attributed to the completion of the $sp \rightarrow d$ electron transfer⁵ and the onset of core repulsions.³⁰ The same steep rise in temperature is not observed in Ca indicating the $sp \rightarrow d$ transition is not complete even at the highest pressure

attained experimentally. Overall, the melting curve of Ba bears a close resemblance to that of Cesium,⁷ except that in the case of the latter the corresponding temperatures and pressures are lower by roughly a half.

In summary, we reported new data for the melting curves

of Mg, Ca, Sr, and Ba. We observed that with increasing atomic number, systematic changes occur in the melting curves that seems to be associated with the transitions observed at room temperature and to the increasing *d*-electron character of these metals.

*Present address: HPCAT, Carnegie Institution of Washington, Advanced Photon Source, Building 434E, Argonne National Laboratory, 8700 S. Cass Ave., Argonne, IL 60439.

¹H. L. Skriver, *Phys. Rev. B* **31**, 1909 (1985).

²R. J. Nelmes, D. R. Allan, M. I. McMahon, and S. A. Belmonte, *Phys. Rev. Lett.* **83**, 4081 (1999).

³M. I. McMahon, T. Bovornratanaraks, D. R. Allan, S. A. Belmonte, and J. R. Nelmes, *Phys. Rev. B* **61**, 3135 (2000).

⁴H. Olijnyk and W. B. Holzapfel, *Phys. Lett. A* **100**, 191 (1984).

⁵M. Winzenick and W. B. Holzapfel, *High-Pressure Science and Technology*, edited by W. Trzeciakowski (World Scientific, Singapore, 1996), p. 384.

⁶K. Takemura, *Phys. Rev. B* **50**, 16 238 (1994).

⁷R. Boehler and C.-S. Zha, *Physica B & C* **139&140**, 233 (1986).

⁸D. A. Young, *Phase Diagram of The Elements* (University of California Press, Berkeley, 1990).

⁹G. C. Kennedy and R. C. Newton, *Solids Under Pressure* (McGraw-Hill, New York, 1963).

¹⁰A. Jayaraman, W. Klement Jr., and G. C. Kennedy, *Phys. Rev.* **132**, 1620 (1964).

¹¹P. A. Urtiew and R. Grover, *J. Appl. Phys.* **48**, 1122 (1977).

¹²M. Winzenick and W. B. Holzapfel, *Phys. Rev. B* **55**, 101 (1997).

¹³R. Boehler, N. V. Bargaen, and A. Chopelas, *J. Geophys.* **95**, 21731 (1990).

¹⁴R. Boehler, *Phys. Earth Planet. Inter.* **96**, 181 (1996).

¹⁵D. Errandonea, R. Boehler, and M. Ross, *Phys. Rev. Lett.* **85**, 3444 (2000).

¹⁶D. Errandonea, B. Schwager, R. Ditz, C. Guessmann, R. Boehler, and M. Ross, *Phys. Rev. B* **63**, 132104 (2001).

¹⁷R. Boehler, *Rev. Geophys.* **38**, 221 (2000).

¹⁸H. K. Mao, J. Xu, and P. M. Bell, *J. Geophys. Res. Solid* **91**, 4673 (1986).

¹⁹A. K. McMahan and J. A. Moriarty, *Phys. Rev. B* **27**, 3235 (1983).

²⁰H. Olijnyk and W. B. Holzapfel, *Phys. Rev. B* **31**, 4682 (1985).

²¹R. Boehler and M. Ross, *Earth Planet. Sci. Lett.* **153**, 267 (1997).

²²J. A. Moriarty and J. D. Althoff, *Phys. Rev. B* **51**, 5609 (1995).

²³J. L. Pelissier, *Phys. Scr.* **34**, 838 (1986).

²⁴R. M. Wentzcovitch and M. L. Cohen, *Phys. Rev. B* **37**, 5571 (1988).

²⁵R. M. Wentzcovitch, *Phys. Rev. B* **50**, 10 358 (1994).

²⁶R. J. Nelmes, M. I. McMahon, D. R. Allan, S. A. Belmonte, and T. Bovornratanaraks, in *Proceedings of the AIRAPT-17*, edited by M. H. Manghnani, W. J. Nellis, and M. F. Nicol (University Press, Hyderabad, 2000), p. 475.

²⁷D. R. Allan, R. J. Nelmes, M. I. McMahon, S. A. Belmonte, and T. Bovornratanaraks, *Rev. High Pressure Sci. Technol.* **7**, 236 (1998).

²⁸J. C. Haygarth, I. C. Getting, and G. C. Kennedy, *J. Appl. Phys.* **38**, 4557 (1967).

²⁹A. Yoneda and A. Endo, *J. Appl. Phys.* **51**, 3216 (1980).

³⁰W. S. Zeng, V. Heine, and O. Jepsen, *J. Phys.: Condens. Matter* **9**, 3489 (1997).